Molecular Cell
Article

YidC and Oxa1 Form Dimeric Insertion Pores on the Translating Ribosome

Rebecca Kohler,[1,6] Daniel Boehringer,[1,6] Basil Greber,[1] Rouven Bingel-Erlenmeyer,[2] Ian Collinson,[3] Christiane Schaffitzel,[4,5,*] and Nenad Ban[1,*]
[1]Institute of Molecular Biology and Biophysics, ETH Zürich, Schafmattstrasse 20, CH-8093 Zürich, Switzerland
[2]Swiss Light Source, CH-5323 Villigen PSI, Switzerland
[3]Department of Biochemistry, University of Bristol, University Walk, BS8 1TD Bristol, UK
[4]Grenoble Outstation, European Molecular Biology Laboratory, 6 rue Jules Horowitz, BP181, 38042 Grenoble Cedex 9, France
[5]Unit of Virus Host-Cell Interactions, UJF-EMBL-CNRS, UMR 5233, 6 rue Jules Horowitz, 38042 Grenoble Cedex 9, France
[6]These authors contributed equally to this work
*Correspondence: ban@mol.biol.ethz.ch (N.B.), schaffitzel@embl.fr (C.S.)
DOI 10.1016/j.molcel.2009.04.019

SUMMARY

The YidC/Oxa1/Alb3 family of membrane proteins facilitates the insertion and assembly of membrane proteins in bacteria, mitochondria, and chloroplasts. Here we present the structures of both *Escherichia coli* YidC and *Saccharomyces cerevisiae* Oxa1 bound to *E. coli* ribosome nascent chain complexes determined by cryo-electron microscopy. Dimers of YidC and Oxa1 are localized above the exit of the ribosomal tunnel. Crosslinking experiments show that the ribosome specifically stabilizes the dimeric state. Functionally important and conserved transmembrane helices of YidC and Oxa1 were localized at the dimer interface by cysteine crosslinking. Both Oxa1 and YidC dimers contact the ribosome at ribosomal protein L23 and conserved rRNA helices 59 and 24, similarly to what was observed for the nonhomologous SecYEG translocon. We suggest that dimers of the YidC and Oxa1 proteins form insertion pores and share a common overall architecture with the SecY monomer.

INTRODUCTION

A large proportion of proteins needs to be incorporated into specific cellular membranes; in *E. coli*, it is about 20%–30% of the total number (Luirink et al., 2005). In bacteria, most nascent inner membrane proteins (IMPs) are recognized by the ubiquitous signal recognition particle (SRP) (Keenan et al., 2001) and targeted to SecYEG, which forms a protein-conducting channel (Brundage et al., 1990; Rapoport, 2007). The energy-transducing membranes of bacteria, mitochondria, and chloroplasts have a high demand for the insertion and assembly of respiratory complexes and ATP synthases. This requires the function of a specific membrane protein "insertase" from the YidC/Oxa1/Alb3 family (Bonnefoy et al., 1994; Luirink et al., 2001; Samuelson et al., 2000; Scotti et al., 2000). In *E. coli*, YidC is essential (Samuelson et al., 2000). It works in conjunction with the canonical SRP-SecYEG pathway and also as a Sec-independent insertase. The latter function is similar to that of Oxa1 in mitochondria, which lack the components of the Sec system (Glick and Von Heijne, 1996).

YidC is involved in membrane protein folding, assembly, and quality control (Beck et al., 2001; Nagamori et al., 2004; van Bloois et al., 2008). In the Sec-dependent pathway, it interacts with transmembrane helices (TMHs) of membrane proteins after their release from the SecYEG translocon (Urbanus et al., 2001; van der Laan et al., 2001), thereby preventing their aggregation. Thus, YidC has been proposed to function as a membrane chaperone (Nagamori et al., 2004). Membrane protein insertion probably occurs cotranslationally, since YidC was found to be associated with nascent Sec-dependent proteins (Froderberg et al., 2004; Samuelson et al., 2000; van der Laan et al., 2001). The interaction of YidC with the SecYEG translocon is thought to be mediated via the accessory complex SecDFYajC (Nouwen and Driessen, 2002). In the membrane, YidC is much more abundant than SecYEG (Driessen, 1994; Urbanus et al., 2002). Therefore, it likely exists both as a complex with SecYEG-SecDFYajC and in an unbound form.

In the Sec-independent pathway, YidC acts in its isolated state and is responsible for the insertion of the F_0 subunit c of the ATP synthase (F_0c), subunit II of the cytochrome o oxidase (CyoA), and the mechanosensitive channel MscL (Facey et al., 2007; van der Laan et al., 2003, 2004). Furthermore, YidC alone is sufficient for the insertion of several small phage proteins (Samuelson et al., 2000; Serek et al., 2004). Substrates of the Sec-independent pathway are typically rather small and often consist of two TMHs connected via a short hairpin (Kiefer and Kuhn, 2007). To date, it has not been firmly established if the Sec-independent insertion route is exclusively cotranslational and whether or not SRP is involved in Sec-independent substrate targeting (Kiefer and Kuhn, 2007).

The YidC/Oxa1/Alb3 family possesses a conserved core of five TMHs, which define the insertase function (Jiang et al., 2003). The importance of the YidC/Oxa1/Alb3 proteins is reflected by their extraordinary functional complementarity, which spans vast evolutionary distances (Jiang et al., 2002; van Bloois et al., 2005, 2007). YidC contains an N-terminal extension to the core insertase consisting of an additional TMH and a large periplasmic domain.

The structural information on YidC is limited to a high-resolution structure of the periplasmic domain (Oliver and Paetzel, 2008; Ravaud et al., 2008) and a 10 Å projection map of the full-length membrane-bound dimer (Lotz et al., 2008). The periplasmic domain adopts a β supersandwich fold with an α-helical and, likely, flexible linker region at the C-terminal end. The N-terminal part of the domain seems to be flexibly linked to the nonessential YidC TMH 1 (Oliver and Paetzel, 2008). In the crystal structure, the periplasmic domain is monomeric, suggesting that YidC dimerization determinants reside in the transmembrane (TM) region of the protein. In the YidC projection structure, a region of lower density was observed at the dimer interface and proposed to be part of the insertion pore (Lotz et al., 2008). Interestingly, YidC TMH 1 and TMH 3 were shown to contact TMHs of YidC substrates (Klenner et al., 2008; Yu et al., 2008; Yuan et al., 2007).

Mitochondria possess neither SRP nor SecYEG (Glick and Von Heijne, 1996), yet they retain a need for a classical, bacterial-like insertion of the mitochondrially encoded proteins, all of them small TM proteins. Therefore, Oxa proteins must serve this function in mitochondria, in addition to facilitating the insertion of those membrane proteins that are imported into the matrix from the cytoplasm, like F_0c homologs (Luirink et al., 2001). The Oxa1 protein contains a C-terminal extension that is required for ribosome binding (Jia et al., 2003). Furthermore, Oxa1 has been crosslinked to Mrp20, the mitochondrial homolog of the *E. coli* ribosomal protein L23, associating it with a cotranslational mechanism of membrane protein insertion (Szyrach et al., 2003).

In spite of the implication that YidC functions cotranslationally, an interaction of YidC with the ribosome has yet to be shown. In this study, we demonstrate that YidC interacts directly with the large ribosomal subunit. We have employed cryo-electron microscopy (cryo-EM) to determine the structures of YidC and Oxa1 bound to *E. coli* ribosomes displaying a nascent chain derived from the Sec-independent substrate F_0c. Our structural and biochemical analyses expose the stoichiometry of the potential pore-forming state of YidC and Oxa1 and underline the remarkable conservation between the two proteins. The results also reveal an unforeseen commonality between the overall architecture and mechanism of the YidC-like and SecY-type protein-conducting channels.

RESULTS

YidC and Oxa1 Interact with Bacterial Ribosomes

Particular substrates of the Sec-independent YidC pathway have been shown to insert cotranslationally (Chen et al., 2002; van der Laan et al., 2004). To investigate this process, we characterized the interactions of YidC with nontranslating ribosomes and with ribosomes displaying the F_0c subunit of F_0F_1 ATPase. The ribosome nascent chain complexes (RNCs) were generated by in vitro translation and purified by sucrose gradient centrifugation followed by affinity chromatography (Schaffitzel and Ban, 2007). The *E. coli* F_0c subunit of the F_0F_1 ATPase was used as a nascent chain bait in all experiments, as F_0c is a well-characterized and promiscuous substrate of both YidC and Oxa1 (van Bloois et al., 2005; van der Laan et al., 2004). The nascent chain construct was designed such that only the first TMH of the F_0c subunit (amino acids 1–79) is displayed on the ribosome, thereby effectively mimicking an insertion intermediate upon binding to the insertase.

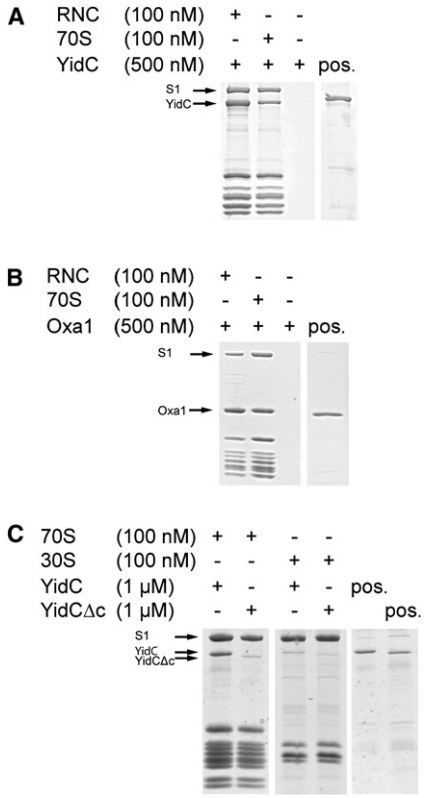

Figure 1. Binding of YidC and Oxa1 to Ribosomes and RNCs Analyzed by Ribosomal Pelleting

Ribosomes or RNCs were incubated with an excess of detergent-purified YidC or Oxa1 variants as indicated. After pelleting by ultracentrifugation, the pellet fraction was analyzed by SDS-PAGE and Coomassie staining. Positive controls were prepared as described in the Experimental Procedures.

(A) Binding of YidC to *E. coli* ribosomes and RNCs. YidC interacts with the ribosome; the binding signal for YidC is stronger for translating than for nontranslating ribosomes. A positive control shows the YidC signal expected for a 2:1 association of YidC with the ribosome.

(B) *S. cerevisiae* Oxa1 interacts with *E. coli* ribosomes. Similarly to the RNC-YidC complex, the interaction between Oxa1 and *E. coli* ribosomes seems to be stabilized by the nascent F_0c polypeptide chain. A positive control shows the Oxa1 signal expected for a 1:1 association of Oxa1 with the ribosome.

(C) The C terminus of YidC is required for ribosome binding. YidC does not cosediment efficiently with small ribosomal subunits, indicating that the binding is mediated by the large ribosomal subunit. Positive controls show the YidC signals expected for a 1:1 association of YidC with the ribosome.

Purified *E. coli* 70S ribosomes or RNCs were incubated with detergent-solubilized, purified YidC (Lotz et al., 2008). Subsequent analysis of cosedimentation pellets after ultracentrifugation confirmed that *E. coli* YidC binds strongly to 70S ribosomes. The ribosome binding was further enhanced by the presence of the substrate nascent chain that additionally interacts with YidC (Figure 1A). Virtually no binding was detected between YidC and the small ribosomal subunit, indicating that the large ribosomal subunit is required for a productive interaction (Figure 1C).

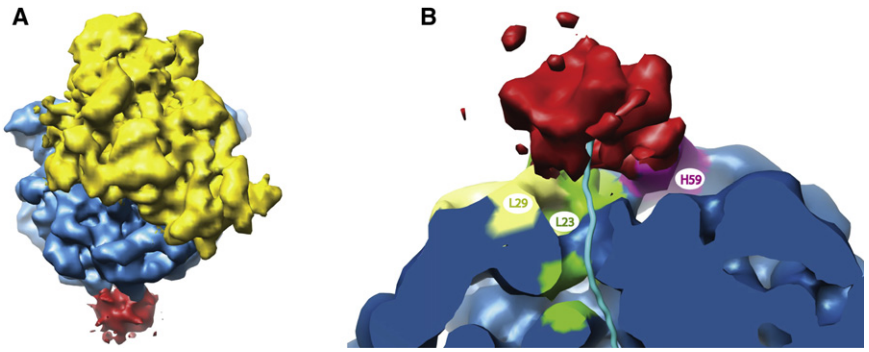

Figure 2. The 3D Structure of YidC in Complex with the Translating Ribosome

(A) Cryo-EM density of the *E. coli* RNC-YidC complex. YidC is bound at the tunnel exit of the RNC. The small subunit is shown in yellow, the large subunit in blue, and the YidC density in red.

(B) The ribosome was cut along the polypeptide tunnel to allow a direct view on the main contact sites of YidC. Ribosomal proteins located in this area are color coded: L23 in green, L29 in yellow, and helix 59 of the 23S rRNA in magenta. The path of the modeled nascent polypeptide chain is shown in cyan; it enters the YidC density at its center.

Oxa1 has been shown to bind to mitochondrial ribosomes (Jia et al., 2003; Szyrach et al., 2003), and it can restore growth in YidC depletion strains by taking over the Sec-independent function of YidC in *E. coli* (van Bloois et al., 2005). Therefore, we tested this functional conservation with respect to the *E. coli* ribosome. Indeed, we were able to establish a stable complex of the yeast mitochondrial Oxa1 with the bacterial ribosome. Similar to the results we obtained for the YidC binding test, Oxa1 binds to ribosomes and RNCs (Figure 1B).

The cytoplasmic loops of YidC contain a number of charged amino acids that could interact with the ribosome. In the case of Oxa1, the positively charged C-terminal domain has been shown to directly interact with the mitochondrial ribosome (Jia et al., 2003; Szyrach et al., 2003). In order to investigate whether the shorter, positively charged C terminus of YidC (amino acids 536–548) could contribute to the ribosome binding in *E. coli*, the last 13 amino acids were deleted. Binding to ribosomes was analyzed by cosedimentation and SDS-PAGE. We found that binding of YidC to ribosomes was reduced to background levels by the deletion of the C terminus (Figure 1C). The interaction with YidC was also lost by increasing the ionic strength (see Figure S1 available online), indicating that binding is mediated by ionic interactions. Furthermore, no significant interaction could be detected to the small ribosomal subunit (Figure 1C). From these data, we conclude that the charged C terminus of YidC mediates important interactions with the large ribosomal subunit.

3D Reconstruction of YidC Bound to the Translating Ribosome

To obtain insight into the structure of the insertase bound to a translating ribosome, we determined the 3D structure of the complex of YidC and a SecM-stalled RNC displaying the F_0c insertion intermediate by cryo-EM (Figure 2A). As a first reference, a low pass filtered model of the *E. coli* RNC was used (Schaffitzel et al., 2006). Comparing the 3D structure of the RNC-YidC complex to the structure of the empty RNC revealed an additional density at the tunnel exit, corresponding to YidC. After supervised classification for RNCs showing the extra density (Figure S2A), the structure of the RNC-YidC complex was refined to a resolution of 14.4 Å (Fourier shell correlation [FSC] 0.5 criterion), comparable to recent reconstructions of SecM-stalled RNCs (Mitra et al., 2005; Schaffitzel et al., 2006). The ribosomal P and E sites are occupied by transfer RNAs (tRNAs), whereas the occupancy of the A site is low. Therefore, the growing polypeptide chain is predominantly attached to the peptidyl-tRNA in the P site.

The YidC density is located above the polypeptide tunnel exit and has a compact, slightly elongated bilobal shape with a diameter of about 70 Å (Figures 2B and 3). The YidC density is shown

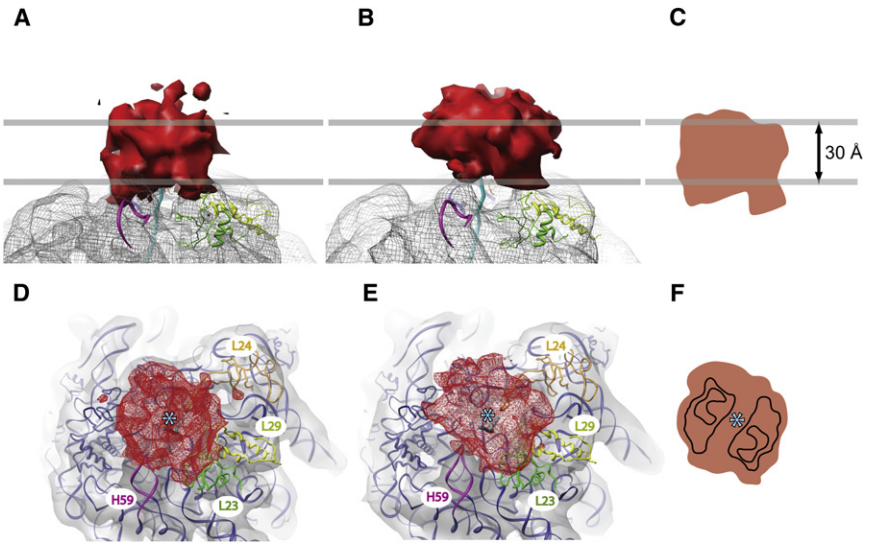

Figure 3. YidC and Oxa1 Bound to the Translating Ribosome

(A and B) Shown is the side view of YidC (A) and Oxa1 (B) (red surfaces) on the bacterial ribosome (gray mesh). The gray lines indicate the membrane boundaries. Ribosomal proteins L23, L29, and L24, as well as helix 59 of the 23S rRNA, are shown for orientation (compare with lower panel).

(C) For comparison, the outline of the YidC density is shown together with the dimension of the plasma membrane.

(D and E) Shown is the top view of YidC (D) and Oxa1 (E) along the ribosomal tunnel.

(F) Superposition of the YidC projection structure (Lotz et al., 2008) onto an outline of the YidC density as shown in (D).

The *E. coli* ribosome crystal structure (Schuwirth et al., 2005) was fitted into the ribosomal cryo-EM density. Ribosomal proteins L23, L29, and L24, as well as helix 59 of the 23S rRNA, are highlighted. The star marks the exit point of the nascent protein chain; its path is highlighted in blue.

at the same threshold level as the RNC, revealing the details of the interaction site. The dimension of the YidC insertase density agrees with the thickness of a lipid bilayer (Figure 3C), which implies that the TM part accounts for most of the EM map. Density corresponding to the probably flexibly linked periplasmic domain of YidC (Oliver and Paetzel, 2008) is not visible. This is not unexpected, since flexible molecule parts are averaged out in the single-particle 3D reconstruction process. The volume enclosed by the density of YidC corresponds to a protein mass of two times the YidC TM portion. Since the YidC density is centered above the tunnel exit, the nascent protein chain, not visualized at this resolution, is likely to enter the YidC density in the middle (Figure 3D). This reconstruction demonstrates a direct interaction between the ribosome, the nascent chain, and the insertase in the Sec-independent YidC insertion pathway.

Three major contact sites were identified between the 50S ribosomal subunit and YidC (Figures 3A and 3D): strong contacts are visible at helix 59 of the 23S ribosomal RNA (rRNA) and ribosomal proteins L23 and L29. The third contact site consists of two thinner connections that are formed at the tip of ribosomal protein L24 and at helix 24 of the 23S rRNA. In comparison to the *E. coli* 70S crystal structure (Schuwirth et al., 2005), helix 59 is displaced toward YidC by 6 Å (Figure 3A). A similar conformational change has been observed in the RNC-SRP complex (9 Å displacement) (Schaffitzel et al., 2006) and in the 70S-SecYEG complex (5 Å displacement) (Menetret et al., 2007), suggesting some similarity in the mode of binding between all of these factors involved in cotranslational protein targeting and translocation. The significance of this conformational change remains to be determined.

The RNC-Oxa1 Complex

To investigate whether, in addition to their functional similarity, *E. coli* YidC and *S. cerevisiae* Oxa1 also share a common architecture and arrangement when in complex with the translating ribosome, we determined the 3D structure of Oxa1 bound to the *E. coli* RNC (Figure S3). Again we used *E. coli* RNCs displaying the F_0c subunit of the F_0F_1 ATP synthase, which is a homolog of the natural Oxa1 substrate Atp9 (Jia et al., 2007).

In the structure of the RNC-Oxa1 complex, the Oxa1 density is centered above the ribosomal tunnel exit. The size (diameter of ~70 Å) and shape of the Oxa1 density are similar to that of YidC (Figures 3A, 3B, 3D, and 3E). The threshold level of the RNC-Oxa1 density was chosen at a similar level used for the RNC-YidC complex. In the EM structure, Oxa1 is positioned similarly with respect to the ribosomal tunnel exit and oriented in the same way as YidC, and the thickness also corresponds to that of a typical helical TM domain (Figure 3C). YidC and Oxa1 share a conserved core of five TM segments, whereas the size of the periplasmic part differs: ~300 residues and ~90 residues for YidC and Oxa1, respectively. Therefore, the similar size of the two insertase densities confirms that the TM core dominates the observed density in both structures (RNC-YidC and RNC-Oxa1).

The contact sites of Oxa1 on the ribosome are identical to that of YidC. A strong contact is visible at L23 and L29 (Figures 3B and 3E). This is consistent with the observation that Oxa1 can be crosslinked to the mitochondrial counterpart of *E. coli* L23, Mrp20 (Jia et al., 2003), probably by means of its ribosome-binding C terminus (Jia et al., 2003; Szyrach et al., 2003). Therefore, the contact at L23 is likely to be formed by the Oxa1 C terminus. The second ribosomal contact site is helix 59 of the 23S rRNA, which is displaced toward Oxa1 as described above for the RNC-YidC complex. The third connection between rRNA helix 24 and Oxa1 is rather weak but can be observed at lower threshold values (data not shown).

Dimers of YidC and Oxa1 Bind to the Ribosome

The dimensions of ribosome-bound YidC match the structure of the membrane-bound form of YidC, which is a dimer (Lotz et al., 2008) (Figure 3F). To further investigate the oligomeric state of YidC alone in solution and in complex with ribosomes, we performed blue native gel electrophoresis (BN PAGE) and chemical crosslinking experiments.

Purified YidC was incubated with increasing concentrations of decyl maltoside (DM) and analyzed by BN PAGE (Figure S4). At the critical micellar concentration (CMC) of DM, a ladder of bands was visible, corresponding to monomer, dimer, and higher oligomeric states. At higher detergent concentrations, YidC migrated predominantly as a monomer with some dimers. When the detergent concentration was lowered again, the monomer reassociated to dimers and higher oligomeric states. Thus, equilibrium exists between YidC monomers and dimers in detergent solution; the additional higher-molecular-weight forms are probably a result of aggregation due to loss of detergent micelles.

In order to assess the oligomeric state of YidC when bound to the translating ribosome, we used the PICUP method utilizing the light-inducible crosslinking reagent tris-bipyridylruthenium (II) ($Ru[bpy]_3$) (Fancy and Kodadek, 1999). Light activation of $Ru(bpy)_3$ together with ammonium persulfate (APS) triggers radical reactions (Fancy and Kodadek, 1999) that induce fast and efficient covalent bond formation only between molecules that are in van der Waals contact. YidC with and without ribosomes and ribosomal subunits was incubated at a detergent concentration of 10× CMC before the PICUP reagents were added and the sample exposed to visible light. Corresponding crosslinking experiments for Oxa1 were performed in parallel.

Analysis of the crosslinked samples showed that solubilized YidC and Oxa1 are primarily monomeric in the detergent concentrations used for EM and sedimentation experiments. In the presence of ribosomes, we observe an increased intensity of the dimer bands of YidC (Figure 4A) and of Oxa1 (Figure 4B). The relative intensities of the dimer bands obtained for YidC and Oxa1 cannot be compared quantitatively, since the two proteins require different sample buffers. In control experiments with the small 30S ribosomal subunit, the very weak intensity of the dimer band corresponds to the intensity observed for the insertase-only sample (Figure 4A). This suggests that the large ribosomal subunit stabilizes the dimer form of the YidC and Oxa1 insertases.

Cysteine Crosslinking of YidC and Oxa1 Dimers

In order to further characterize the dimerization interface of the conserved TM part of YidC and Oxa1, we assessed the vicinity of cysteines in opposing monomers by their ability to be oxidized

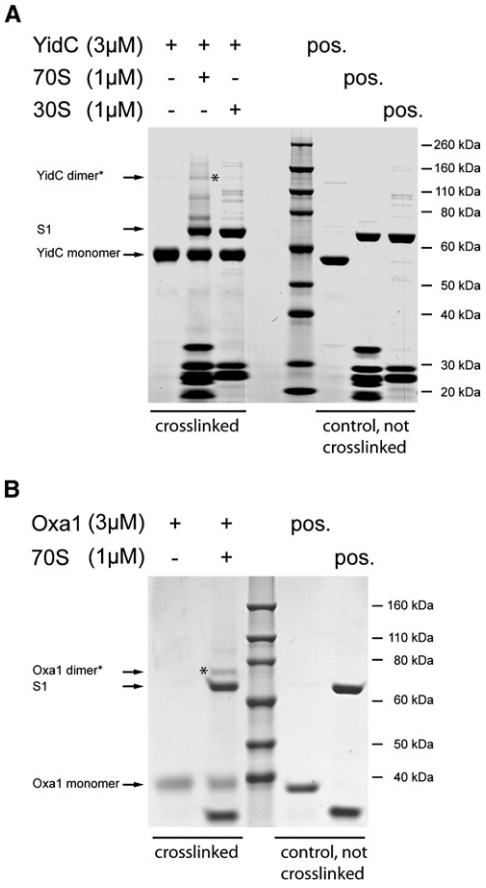

Figure 4. The Ribosome Stabilizes Dimeric Forms of YidC and Oxa1

$(Ru[bpy]_3)_2$ crosslinking of the RNC-YidC and RNC-Oxa1 complexes. Ribosomes (1 μM) were incubated with a 3-fold molar excess of YidC or Oxa1, 4 mM APS, and 0.2 mM $(Ru[bpy]_3)_2$ prior to photoactivation. The crosslinked samples were analyzed by SDS-PAGE and Coomassie staining. The identity of the YidC and Oxa1 dimer bands (star) was confirmed by mass spectrometry. Control samples to the right of the marker bands were not crosslinked.

(A) In the presence of ribosomes, a YidC dimer band appears, while in the 30S sample and the ribosome-free control, almost no dimer can be observed.

(B) Similar to YidC, Oxa1 dimer formation could be observed in the presence of *E. coli* ribosomes.

and crosslinked to one another. YidC and Oxa1 each contain a single conserved cysteine. Cysteine 423, located in TMH 3 of YidC (Figure 5C), has been shown to crosslink to the nascent chain (van der Laan et al., 2001), indicating that it could be part of a potential insertion pore.

Purified YidC was incubated with or without ribosomes. Copper phenanthroline was used as a hydrophobic oxidizing agent, and the products were visualized by SDS-PAGE. For solubilized YidC, a weak dimer band could be observed (Figure 5A); if ribosomes were added, the fraction of molecules forming dimers increased considerably. This is in agreement with the $Ru(bpy)_3$ crosslinking experiments suggesting that the ribosome induces dimerization or stabilizes the dimeric form of YidC.

Cysteines can only be crosslinked if the distance between the β carbons is ~4.5 Å (Vinayagam et al., 2004), indicating that the two TMH 3 helices are very close to each other at the YidC dimer interface. Combining our cysteine crosslinking result with the finding that the nascent polypeptide chain contacts TMH 3 of YidC near C423 (Yu et al., 2008) suggests a positioning of the nascent chain in the center of the YidC dimer. The experiment was repeated with Oxa1 (Figure 5B). Here, the single cysteine is located in TMH 1 (Figure 5C), corresponding to TMH 2 in YidC. Alone, Oxa1 after oxidation was mostly in a monomeric form. In the presence of ribosomes, most Oxa1 is crosslinked as a dimer. Therefore, TMH 1 of Oxa1 also forms part of the dimer interface. Assuming that the 3D arrangement of the conserved TMH core of YidC and Oxa1 is similar, our results imply that the two conserved TMHs 2 and 3 of YidC (corresponding to TMHs 1 and 2 in Oxa1) form the central core of the dimer and are in close proximity to their counterparts in the second YidC molecule (Figure 5D). This also suggests that the two YidC molecules dimerize in a head-to-tail organization, also indicated by the arrangement of YidC molecules in the membrane (Lotz et al., 2008).

DISCUSSION

Here we report the structures determined by cryo-EM of YidC and Oxa1 bound at the polypeptide tunnel exit of translating bacterial ribosomes. The data show that the active form of the insertases is conserved and dimeric. The attachment sites on the ribosome are also consistent between YidC and Oxa1 and are shared by the nonhomologous SecYEG translocon. This astonishing similarity, shared by bacteria, mitochondria, and presumably also chloroplast (Alb3) membrane insertion factors (Jiang et al., 2002) suggests a common architecture for protein insertion and translocation.

The mitochondrial and *E. coli* insertases share a conserved core of five TM segments (Figure 5C); Oxa1 lacks TMH 1 and the large periplasmic domain of YidC but has an extended, highly positively charged C terminus. The latter is important for insertion of nascent chains and makes a direct contact with mitochondrial ribosomes (Jia et al., 2003; Szyrach et al., 2003). Removal of the shorter, also positively charged C terminus in YidC reduces the affinity of binding such that a stoichiometric RNC-YidC complex can no longer be observed in cosedimentation experiments. However, a C-terminally truncated YidC retained activity in vivo, indicating that other parts of the protein, as well as the substrate nascent polypeptide chain, provide weaker but sufficient interaction sites for ribosome binding (Jiang et al., 2003), all consistent with the multiple contacts observed in the structure. In addition, the SRP/FtsY system could contribute to targeting of YidC substrates to the insertase (Kiefer and Kuhn, 2007). In mitochondria, in the absence of the SRP/FtsY system, the extension of the Oxa1 C terminus might provide additional affinity to mitochondrial ribosomes.

As the size and shape of the YidC and Oxa1 densities are similar, the density corresponds to the conserved TMH core. Thus, the large periplasmic domain of YidC that is probably flexibly connected to the TM part (Oliver and Paetzel, 2008) was not resolved. This suggests that, due to its direct interactions with the ribosome, the TM domain is ordered while the peripheral features are somewhat flexible, a feature also apparent in the projection map of the membrane-bound YidC (Lotz et al.,

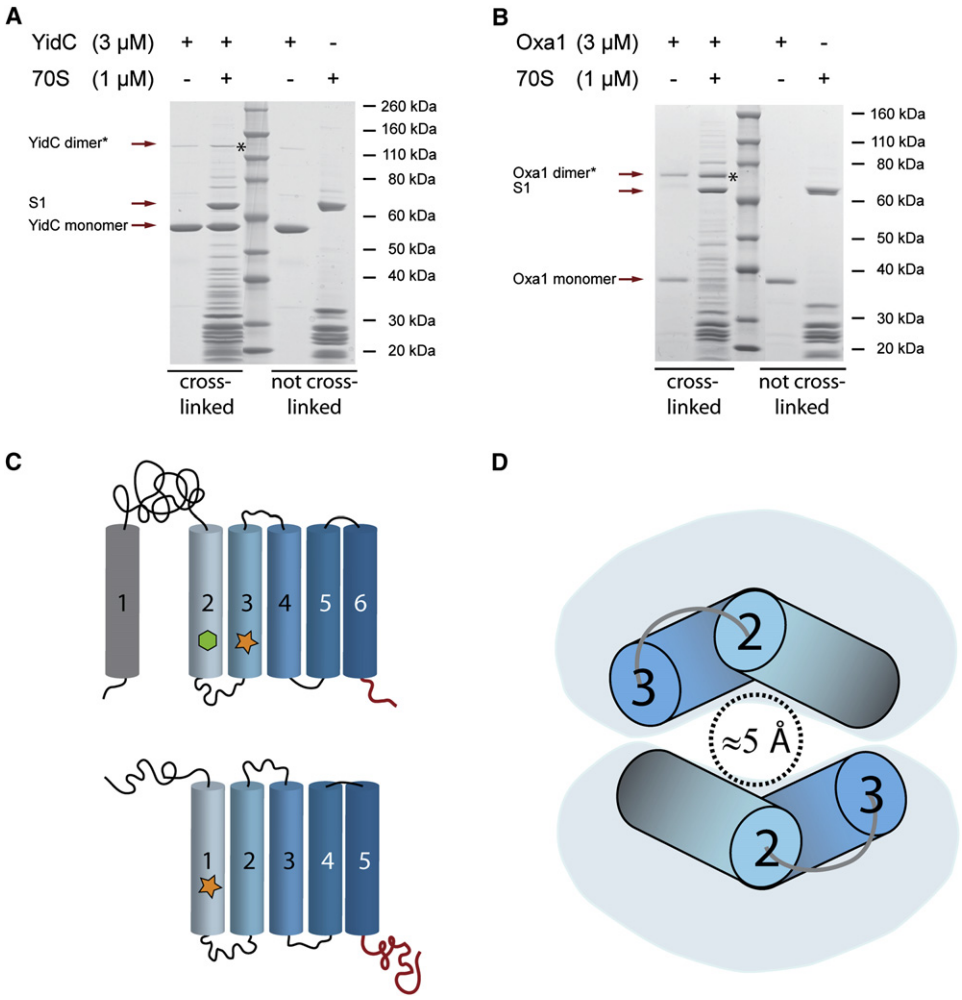

Figure 5. TMHs 2 and 3 of YidC Likely Contribute to an Insertion Pore, as Shown by Cu-Phenanthroline Oxidation of Cysteines

(A and B) YidC (A) and Oxa1 (B) can be crosslinked as dimers by disulfide oxidation. Samples were analyzed by SDS-PAGE and Coomassie staining. The identity of the YidC and Oxa1 dimer bands (star) was confirmed by mass spectrometry.

(C) Topology models of YidC (above) and Oxa1 (below). The conserved five TMH core is shown in blue and the positively charged C termini in red. Homologous helices are colored similarly. The position of the natural YidC cysteine C423 is shown as an orange star. YidC T362 is marked with a green hexagon. It is thought to be in close proximity to C423 (see the Discussion) (Yuan et al., 2007). The natural Oxa1 cysteine C141 is marked with an orange star; its corresponding residue in the YidC molecule is I368.

(D) Arrangement of the TM helices in the center of a YidC dimer. Assuming the 3D arrangement of the conserved TMH core is similar in YidC and Oxa1, both conserved helices TMH 2 and TMH 3 form the core of the dimer center and contact their counterparts in the second YidC molecule, thereby possibly contributing residues to an insertion pore. The distance between the C_β atoms of two crosslinked cysteines must be 5 Å or less.

2008). Indeed, our solution structures and the projection map are compatible with each other and define a dimer formed by the TM portion of the molecule.

The active SecYEG complex is probably formed by membrane-bound dimers (Bessonneau et al., 2002; Breyton et al., 2002). However, only one of them is active at any one time during posttranslational translocation (Osborne and Rapoport, 2007). In view of the mixed reports regarding the oligomeric state of SecY in translocon-ribosome complexes (Menetret et al., 2007; Mitra et al., 2005; Rapoport, 2008), we decided to investigate the stoichiometry of the YidC and Oxa1 in complex with the ribosome using crosslinking in addition to the obtained structural data.

Photochemical and oxidative crosslinking experiments demonstrate that once again YidC and Oxa1 behave in the same way. Both experiments identify dimers that are stabilized by the large ribosomal subunit. Photochemical crosslinking using the PICUP method allowed us to detect the oligomeric state of the insertases under near-equilibrium conditions. The formation of the intermolecular disulfide bonds between the naturally occurring cysteines in the YidC and Oxa1 proteins were particularly informative, as they implicate specific TM segments at the dimer interface. Each protein contains a single natural cysteine, YidC in TMH 3 and Oxa1 in TMH 1 (equivalent to TMH 2 of YidC) (Figure 5C). Genetic studies indicate the importance of YidC TMH 3 and its close proximity to TMH 2 (Yuan et al., 2007). YidC T362E

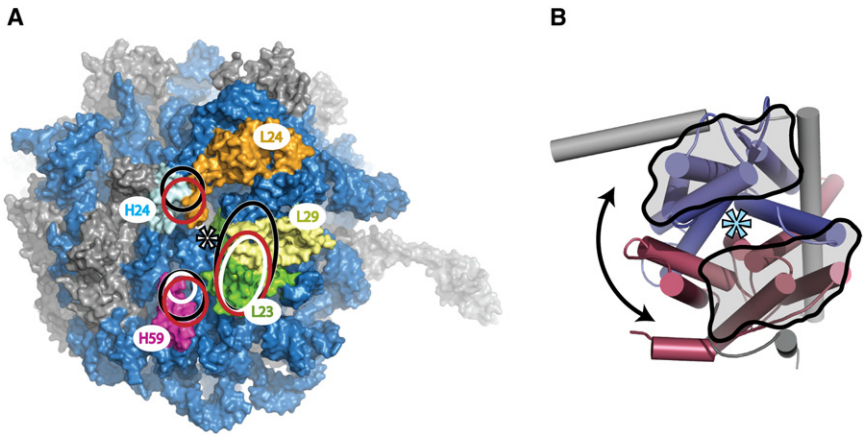

Figure 6. Comparison of YidC, Oxa1, and SecYEG Bound to Ribosomes

(A) Contact areas of YidC, Oxa1, and SecYEG on the ribosome. The docking regions of the three insertases are highlighted as follows: YidC in red, Oxa1 in white, and SecYEG in black. Helix 59 (H59) of the 23S rRNA is a contact point for all three insertases, as well as the L23/L29 region. YidC and SecYEG have an additional strong anchor point at L24/H24, whereas Oxa1 shows only a weak connection in this area. Ribosomal proteins are shown in gray and rRNA in blue. The following proteins and RNA regions are highlighted: L23 (green), L29 (yellow), L24 (orange), helix 59 (magenta), and helix 24 (cyan) of the 23S rRNA.

(B) Superposition of the YidC dimer projection structure (Lotz et al., 2008) with the SecYEβ translocon crystal structure (Van den Berg et al., 2004). The YidC dimer is similar in size to the SecYEβ translocon. The crab's claw-like opening movement of SecYEβ is indicated by an arrow. The stars indicate the tunnel exit.

(in TMH 2) was identified as an intragenic suppressor that overcame the cold sensitivity of the C423R mutation (in TMH 3), probably by forming an ion pair (Figure 5C). Therefore, TMHs 2 and 3 of YidC must be very close to each other and to their counterparts in the other ribosome-associated monomer. In this respect, it is particularly interesting that the nascent chain contacts TMH 3 (Yu et al., 2008). Thus, these four helices appear to form part of an insertion pore in YidC (Figure 5D). The results also imply that the insertase dimer has a head-to-tail organization with TMH 2 and TMH 3 in the center, as already suggested by the 2D projection map. This is consistent with the position of the tunnel exit in the RNC-YidC complex where the nascent chain emerges beneath the center of the YidC dimer (Figures 3D and 3F).

The cryo-EM map shows that the TM segments of both YidC and Oxa1 are anchored to the ribosome by three contact sites. The main connection stabilizing the interaction between YidC and the ribosome may involve the 13 residue short, positively charged C terminus of YidC. As high-affinity binding is salt sensitive, the association is most likely mediated by ionic interactions. The strongest connection in the L23/L29 region of the RNC-Oxa1 complex is possibly meditated by the Oxa1 C terminus, as the biochemical data imply (Jia et al., 2003; Szyrach et al., 2003). An Oxa1-like C-terminal extension is also found in YidC of the bacteria *Rhodopirellula baltica* (Kiefer and Kuhn, 2007) and *Streptococcus mutans* (Dong et al., 2008). Therefore, it probably contacts areas that are conserved between bacterial and mitochondrial ribosomes, like L23.

The three contact points of YidC and Oxa1 with the ribosome are the same ones used by the SecYEG translocon (Menetret et al., 2007; Mitra et al., 2005) (Figure 6A). All of them contact and perturb helix 59 of the 23S rRNA (Menetret et al., 2007) and interact with a second site close to L23/L29. The latter region is a particularly frequently used docking site, as it is involved in the interactions of several factors involved in cotranslational folding, targeting, and translocation (Merz et al., 2008; Schaffitzel et al., 2006). A third connection for YidC and SecYEG is visible at L24 and helix 24 of the 23S rRNA but is very weak in the RNC-Oxa1 structure.

Nascent chain substrates of the SecYEG translocon insert between two pseudosymmetric halves of the SecY subunit (TMHs 1–5 and TMHs 6–10) (Van den Berg et al., 2004). The two lobes may open like a crab's claw and thereby form a lateral gate for the passage of TM segments into the lipid bilayer. A superposition of the projection structure of YidC (Lotz et al., 2008) with the crystal structure of the archeal Sec complex (Van den Berg et al., 2004) reveals the remarkably similar size of the SecYEβ complex and a YidC dimer, each consisting of 12 TMHs (Figure 6B). The two structures can be arranged such that the orientations of the respective "half channels" match. Therefore, we propose that the two YidC molecules in the dimer could function in a similar way to the two halves of SecY (Van den Berg et al., 2004), with a channel in the center that opens by a separation of the component halves. The area of low density close to the interface in the YidC (Lotz et al., 2008) monomer may contribute to such a channel. In the Sec-independent pathway, YidC could directly bind its substrates and act analogously to SecYEG. Conversely, the results obtained for YidC suggest that although a dimer of SecYEG has been visualized bound to a translating ribosome (Mitra et al., 2005), it is possible that only one copy of SecYEG is active in cotranslational protein translocation in a mechanism analogous to what was observed for posttranslational translocation (Osborne and Rapoport, 2007).

In the Sec-dependent pathway, YidC most likely acts downstream of SecYEG (van der Laan et al., 2001). Based on our structures, the ribosome-associated SecYEG translocon would preclude the binding of YidC. In this case, the interaction between SecYEG and YidC is probably mediated by the SecD/F/YajC complex (Nouwen and Driessen, 2002). A mechanism could be envisaged whereby substrate molecules are passed on laterally from the SecYEG translocon to the interface of the YidC dimer.

Using a combination of cryo-EM and biochemical methods, we show a remarkable similarity between the YidC-like protein insertases and the SecYEG translocon. Since there is no evidence that SecYEG and the YidC/Oxa1/Alb3 protein family are related by evolution, their common mode of ribosome binding may be a consequence of their related function in

cotranslational insertion of nascent protein chains into a membrane. The results reported here provide the structural basis for additional biochemical and genetic experiments on this system and pave the way toward future understanding of YidC- and Oxa1-mediated protein insertion at high resolution.

EXPERIMENTAL PROCEDURES

Construction of the F_oc Nascent Chain Construct

The pUC19 Vector (Fermentas) was used as a scaffold for an IPTG-induced expression construct as described previously (Schaffitzel and Ban, 2007). An N-terminal triple Strep tag is followed by the first 46 residues of *E. coli* F_oc (the c subunit of the F_oF_1 ATPase F_o sector) and residues 132–170 of *E. coli* SecM including the 17 amino acid SecM stalling sequence (Nakatogawa and Ito, 2002).

Recombinant Protein Expression

The YidC gene was amplified from genomic DNA of *E. coli*, whereas an Oxa1 library plasmid was generously provided by M. Peter to serve as a PCR template.

The gene encoding wild-type *E. coli* YidC (1644 bp) was cloned with a C-terminal hexahistidine (His_6) tag into a pET expression Vector (pET24a_$YidC_{His6}$, Novagen). N-terminally His_6-tagged variants pProEx_$_{His6}$YidC and pProEx_$_{His6}$YidCΔc were obtained by cloning the wild-type YidC gene or fragment bp 1–1605 of the wild-type gene, respectively, into the pProExHtb B vector (Invitrogen).

C-terminally His_6- and Myc-tagged variants (pBAD/Myc-His_$YidC_{Myc-His6}$) were produced by cloning wild-type YidC (1644 bp) into pBAD/Myc-His (Invitrogen).

pET24a_ec$Oxa1_{His6}$ (Novagen) was obtained by cloning bp 127–1210 of the wild-type *S. cerevisiae* Oxa1 gene, which corresponds to the amino acid sequence of the mature Oxa1 protein after cleavage of the mitochondrial targeting sequence, into the pET24a expression vector.

Expression conditions were similar for all pET24a constructs. Plasmids were transformed into *E. coli* strain BL21 (DE3) by electroporation. Cells were grown in TB medium at 37°C and induced with 100 μM IPTG at an OD_{600} of 1.6. The induced culture was grown for another 12–15 hr at 25°C.

E. coli C43 cells harboring the pBAD construct were grown by shaking at 37°C in 2× YT broth containing 100 μg/ml ampicillin. Overexpression was induced with 0.2% arabinose once the cells had reached an exponential phase of growth, and the cells were harvested by centrifugation after 3 hr.

Membrane Preparation and Purification of YidC and Oxa1 Variants

Preparation of the YidC variants was done as described before using 0.2% w/v n-decyl β-D-maltoside (DM) in the final buffer (Lotz et al., 2008). Membranes containing the Oxa1 construct were extracted with 1% w/v n-dodecyl β-D-maltoside (DDM) for 30 min at 4°C. The protein was purified by Ni chelating and size exclusion chromatography in a manner similar to the procedure for the YidC variants and isolated in buffer C (20 mM ADA [pH 6.4], 150 mM NaCl, 0.1% w/v DDM).

Preparation of *E. coli* Ribosome Nascent Chain Complexes

RNCs were prepared as described (Schaffitzel and Ban, 2007). After the final ultracentrifugation step, the pellet containing the RNCs was dissolved in buffer R (20 mM HEPES-KOH [pH 7.5], 200 mM NaCl, 25 mM $MgOAc_2$) and flash frozen at a concentration of 1 μM. Before use, DM or DDM was added to a final concentration of 0.2% or 0.1% as required. RNCs for binding assays were purified by affinity chromatography only (Schaffitzel and Ban, 2007).

Sedimentation Assays

E. coli RNCs (100–420 nM), 70S ribosomes, or 30S ribosomal subunits (stored in buffer R) were incubated with different ratios of YidC and Oxa1 proteins in buffer A or C, respectively; supplemented with 25 mM $MgOAc_2$ for 1 hr on ice; and then centrifuged for 3 hr to pellet the bound protein together with ribosomes/ribosomal subunits. In the negative controls, ribosomes were replaced by the same volume of buffer R supplemented with 0.2% DM or 0.1% DDM.

The pellets or tube bottoms were washed once with buffer A or C, resuspended in 15 μl 1× SDS gel loading buffer, and analyzed by SDS-PAGE and subsequent Coomassie staining. Positive controls were also applied and consisted of YidC, Oxa1, or ribosomes dissolved in 1× gel loading buffer.

PICUP Crosslinking Assays

Samples containing YidC or Oxa1 were crosslinked by the PICUP method (Fancy and Kodadek, 1999). The buffer conditions were similar to those used in sedimentation assays; the total sample volume was 10 μl. Samples were mixed and incubated for 30 min on ice. APS (4 mM) and 0.2 mM Tris-bipyridylruthenium(II) were added to the mixture, and the proteins were crosslinked by irradiation for 10–30 s with a 250 W slide projector lamp at a distance of 20 cm. The reaction was quenched by addition of 200 mM DTT, and the samples were analyzed by 4%–12% gradient SDS-PAGE (Invitrogen) and Coomassie staining.

Disulfide Crosslinking Assays

Samples were prepared similarly to the protocol used for the PICUP crosslinking procedure. After the incubation step, copper phenanthroline was added to a total concentration of 2 mM and incubated for 15 min at room temperature. The reaction products were analyzed by nonreducing SDS-PAGE and subsequent Coomassie staining.

Cryo-Electron Microscopy and Single-Particle Reconstruction

Sample preparation for cryo-EM was similar to that for sedimentation assays. The concentration of *E. coli* RNCs was 100 nM, and YidC or Oxa1 were added in an 8- to 12-fold excess. The samples were incubated for 30 min on ice, applied to a carbon coated grid, and vitrified by plunging into liquid ethane (Dubochet et al., 1988). The grids were kept at liquid nitrogen temperature and imaged in a FEI F20 microscope (FEI, Hillsboro, OR) at a magnification of 50,000× with an acceleration voltage of 200 kV. Micrographs were recorded on Kodak SO-163 film (Eastman Kodak, Rochester, NY) under low dose conditions at 1.0–4.0 μm defocus. The images were scanned with a CCD scanner (Super Coolscan 9000 ED, Nikon Corporation, Tokyo, Japan) at a step size of 12.7 μm and coarsened to a final pixel size of 3.17 Å on the object scale. The RNC-YidC data set consisted of a total of 45,970 single-particle images, which were CTF corrected (Sander et al., 2003) and used for image processing with the Imagic-5 software (van Heel et al., 1996). Briefly, after an alignment procedure using an RNC structure without bound factor as an initial reference (Schaffitzel et al., 2006), images were subjected to a multivariate statistical analysis (van Heel and Frank, 1981) and classification. The class averages were used for 3D structure determination by the angular reconstitution approach to calculate an initial structure. Final rounds of refinement were done using the Spider software (Frank et al., 1996). We used a supervised classification procedure (Figure S2A) to select for RNCs with stably bound P and E site tRNAs and bound YidC (24,395 particles or 53% of the total number of particles) (Valle et al., 2002). In the case of Oxa1, we used supervised classification (Figure S2B) to select for intact ribosomes with bound Oxa1 (8814 particles or 46% of total particle number). The resolution of the RNC-YidC structure was calculated by the FSC function using the 0.5 criterion and 0.143 criterion to be 15.4 Å and 11.2 Å (Figure S5A), respectively, for data half sets corresponding to an extrapolated resolution of 14.4 Å and 11.0 Å for the full data set (LeBarron et al., 2008). Likewise, the resolution of the RNC-Oxa1 complex was estimated to be to be 18.4 Å and 14.4 Å for data half sets (Figure S5B) corresponding to 18.1 Å and 14.2 Å for the full data set. Structural figures were prepared with Chimera (Pettersen et al., 2004).

ACCESSION NUMBERS

The structures of the RNC-YidC and RNC-Oxa1 complexes have been deposited in the Electron Microscopy Database under accession numbers EMD-1615 and EMD-1616, respectively.

SUPPLEMENTAL DATA

The Supplemental Data include five figures and Supplemental References and can be found with this article online at http://www.cell.com/molecular-cell/supplemental/S1097-2765(09)00272-X.

ACKNOWLEDGMENTS

The authors would like to thank all members of the Ban laboratory for discussions; S. Benke for support; and C. Frick and N. Doerwald for technical assistance. We are grateful to A. Robson for her valuable expertise and to T. Maier for discussion and critical reading of the manuscript. We thank the Electron Microscopy Center Zurich (EMEZ) for support. D.B. was supported by a Federation of European Biochemical Societies Long-Term Fellowship. This work was supported by the Swiss National Science Foundation (SNSF) (to N.B.) and the National Center of Excellence in Research (NCCR) Structural Biology program of the SNSF (to N.B.).

Received: January 28, 2009
Revised: March 9, 2009
Accepted: April 16, 2009
Published: May 14, 2009

REFERENCES

Beck, K., Eisner, G., Trescher, D., Dalbey, R.E., Brunner, J., and Muller, M. (2001). YidC, an assembly site for polytopic *Escherichia coli* membrane proteins located in immediate proximity to the SecYE translocon and lipids. EMBO Rep. *2*, 709–714.

Bessonneau, P., Besson, V., Collinson, I., and Duong, F. (2002). The SecYEG preprotein translocation channel is a conformationally dynamic and dimeric structure. EMBO J. *21*, 995–1003.

Bonnefoy, N., Chalvet, F., Hamel, P., Slonimski, P.P., and Dujardin, G. (1994). OXA1, a *Saccharomyces cerevisiae* nuclear gene whose sequence is conserved from prokaryotes to eukaryotes controls cytochrome oxidase biogenesis. J. Mol. Biol. *239*, 201–212.

Breyton, C., Haase, W., Rapoport, T.A., Kuhlbrandt, W., and Collinson, I. (2002). Three-dimensional structure of the bacterial protein-translocation complex SecYEG. Nature *418*, 662–665.

Brundage, L., Hendrick, J.P., Schiebel, E., Driessen, A.J., and Wickner, W. (1990). The purified *E. coli* integral membrane protein SecY/E is sufficient for reconstitution of SecA-dependent precursor protein translocation. Cell *62*, 649–657.

Chen, M., Samuelson, J.C., Jiang, F., Muller, M., Kuhn, A., and Dalbey, R.E. (2002). Direct interaction of YidC with the Sec-independent Pf3 coat protein during its membrane protein insertion. J. Biol. Chem. *277*, 7670–7675.

Dong, Y., Palmer, S.R., Hasona, A., Nagamori, S., Kaback, H.R., Dalbey, R.E., and Brady, L.J. (2008). Functional overlap but lack of complete cross-complementation of *Streptococcus mutans* and *Escherichia coli* YidC orthologs. J. Bacteriol. *190*, 2458–2469.

Driessen, A.J. (1994). How proteins cross the bacterial cytoplasmic membrane. J. Membr. Biol. *142*, 145–159.

Dubochet, J., Adrian, M., Chang, J.J., Homo, J.C., Lepault, J., McDowall, A.W., and Schultz, P. (1988). Cryo-electron microscopy of vitrified specimens. Q. Rev. Biophys. *21*, 129–228.

Facey, S.J., Neugebauer, S.A., Krauss, S., and Kuhn, A. (2007). The mechanosensitive channel protein MscL is targeted by the SRP to the novel YidC membrane insertion pathway of *Escherichia coli*. J. Mol. Biol. *365*, 995–1004.

Fancy, D.A., and Kodadek, T. (1999). Chemistry for the analysis of protein-protein interactions: rapid and efficient cross-linking triggered by long wavelength light. Proc. Natl. Acad. Sci. USA *96*, 6020–6024.

Frank, J., Radermacher, M., Penczek, P., Zhu, J., Li, Y., Ladjadj, M., and Leith, A. (1996). SPIDER and WEB: processing and visualization of images in 3D electron microscopy and related fields. J. Struct. Biol. *116*, 190–199.

Froderberg, L., Houben, E.N., Baars, L., Luirink, J., and de Gier, J.W. (2004). Targeting and translocation of two lipoproteins in *Escherichia coli* via the SRP/Sec/YidC pathway. J. Biol. Chem. *279*, 31026–31032.

Glick, B.S., and Von Heijne, G. (1996). *Saccharomyces cerevisiae* mitochondria lack a bacterial-type sec machinery. Protein Sci. *5*, 2651–2652.

Jia, L., Dienhart, M., Schramp, M., McCauley, M., Hell, K., and Stuart, R.A. (2003). Yeast Oxa1 interacts with mitochondrial ribosomes: the importance of the C-terminal region of Oxa1. EMBO J. *22*, 6438–6447.

Jia, L., Dienhart, M.K., and Stuart, R.A. (2007). Oxa1 directly interacts with Atp9 and mediates its assembly into the mitochondrial F1Fo-ATP synthase complex. Mol. Biol. Cell *18*, 1897–1908.

Jiang, F., Yi, L., Moore, M., Chen, M., Rohl, T., Van Wijk, K.J., De Gier, J.W., Henry, R., and Dalbey, R.E. (2002). Chloroplast YidC homolog Albino3 can functionally complement the bacterial YidC depletion strain and promote membrane insertion of both bacterial and chloroplast thylakoid proteins. J. Biol. Chem. *277*, 19281–19288.

Jiang, F., Chen, M., Yi, L., de Gier, J.W., Kuhn, A., and Dalbey, R.E. (2003). Defining the regions of *Escherichia coli* YidC that contribute to activity. J. Biol. Chem. *278*, 48965–48972.

Keenan, R.J., Freymann, D.M., Stroud, R.M., and Walter, P. (2001). The signal recognition particle. Annu. Rev. Biochem. *70*, 755–775.

Kiefer, D., and Kuhn, A. (2007). YidC as an essential and multifunctional component in membrane protein assembly. Int. Rev. Cytol. *259*, 113–138.

Klenner, C., Yuan, J., Dalbey, R.E., and Kuhn, A. (2008). The Pf3 coat protein contacts TM1 and TM3 of YidC during membrane biogenesis. FEBS Lett. *582*, 3967–3972.

LeBarron, J., Grassucci, R.A., Shaikh, T.R., Baxter, W.T., Sengupta, J., and Frank, J. (2008). Exploration of parameters in cryo-EM leading to an improved density map of the *E. coli* ribosome. J. Struct. Biol. *164*, 24–32.

Lotz, M., Haase, W., Kuhlbrandt, W., and Collinson, I. (2008). Projection structure of yidC: a conserved mediator of membrane protein assembly. J. Mol. Biol. *375*, 901–907.

Luirink, J., Samuelsson, T., and de Gier, J.W. (2001). YidC/Oxa1p/Alb3: evolutionarily conserved mediators of membrane protein assembly. FEBS Lett. *501*, 1–5.

Luirink, J., von Heijne, G., Houben, E., and de Gier, J.W. (2005). Biogenesis of inner membrane proteins in *Escherichia coli*. Annu. Rev. Microbiol. *59*, 329–355.

Menetret, J.F., Schaletzky, J., Clemons, W.M., Jr., Osborne, A.R., Skanland, S.S., Denison, C., Gygi, S.P., Kirkpatrick, D.S., Park, E., Ludtke, S.J., et al. (2007). Ribosome binding of a single copy of the SecY complex: implications for protein translocation. Mol. Cell *28*, 1083–1092.

Merz, F., Boehringer, D., Schaffitzel, C., Preissler, S., Hoffmann, A., Maier, T., Rutkowska, A., Lozza, J., Ban, N., Bukau, B., and Deuerling, E. (2008). Molecular mechanism and structure of Trigger Factor bound to the translating ribosome. EMBO J. *27*, 1622–1632.

Mitra, K., Schaffitzel, C., Shaikh, T., Tama, F., Jenni, S., Brooks, C.L., 3rd, Ban, N., and Frank, J. (2005). Structure of the *E. coli* protein-conducting channel bound to a translating ribosome. Nature *438*, 318–324.

Nagamori, S., Smirnova, I.N., and Kaback, H.R. (2004). Role of YidC in folding of polytopic membrane proteins. J. Cell Biol. *165*, 53–62.

Nakatogawa, H., and Ito, K. (2002). The ribosomal exit tunnel functions as a discriminating gate. Cell *108*, 629–636.

Nouwen, N., and Driessen, A.J. (2002). SecDFyajC forms a heterotetrameric complex with YidC. Mol. Microbiol. *44*, 1397–1405.

Oliver, D.C., and Paetzel, M. (2008). Crystal structure of the major periplasmic domain of the bacterial membrane protein assembly facilitator YidC. J. Biol. Chem. *283*, 5208–5216.

Osborne, A.R., and Rapoport, T.A. (2007). Protein translocation is mediated by oligomers of the SecY complex with one SecY copy forming the channel. Cell *129*, 97–110.

Pettersen, E.F., Goddard, T.D., Huang, C.C., Couch, G.S., Greenblatt, D.M., Meng, E.C., and Ferrin, T.E. (2004). UCSF Chimera—a visualization system for exploratory research and analysis. J. Comput. Chem. *25*, 1605–1612.

Rapoport, T.A. (2007). Protein translocation across the eukaryotic endoplasmic reticulum and bacterial plasma membranes. Nature *450*, 663–669.

Rapoport, T.A. (2008). Protein transport across the endoplasmic reticulum membrane. FEBS J. *275*, 4471–4478.

Ravaud, S., Stjepanovic, G., Wild, K., and Sinning, I. (2008). The crystal structure of the periplasmic domain of the *Escherichia coli* membrane protein insertase YidC contains a substrate binding cleft. J. Biol. Chem. *283*, 9350–9358.

Samuelson, J.C., Chen, M., Jiang, F., Moller, I., Wiedmann, M., Kuhn, A., Phillips, G.J., and Dalbey, R.E. (2000). YidC mediates membrane protein insertion in bacteria. Nature *406*, 637–641.

Sander, B., Golas, M.M., and Stark, H. (2003). Automatic CTF correction for single particles based upon multivariate statistical analysis of individual power spectra. J. Struct. Biol. *142*, 392–401.

Schaffitzel, C., and Ban, N. (2007). Generation of ribosome nascent chain complexes for structural and functional studies. J. Struct. Biol. *158*, 463–471.

Schaffitzel, C., Oswald, M., Berger, I., Ishikawa, T., Abrahams, J.P., Koerten, H.K., Koning, R.I., and Ban, N. (2006). Structure of the *E. coli* signal recognition particle bound to a translating ribosome. Nature *444*, 503–506.

Schuwirth, B.S., Borovinskaya, M.A., Hau, C.W., Zhang, W., Vila-Sanjurjo, A., Holton, J.M., and Cate, J.H. (2005). Structures of the bacterial ribosome at 3.5 Å resolution. Science *310*, 827–834.

Scotti, P.A., Urbanus, M.L., Brunner, J., de Gier, J.W., von Heijne, G., van der Does, C., Driessen, A.J., Oudega, B., and Luirink, J. (2000). YidC, the *Escherichia coli* homologue of mitochondrial Oxa1p, is a component of the Sec translocase. EMBO J. *19*, 542–549.

Serek, J., Bauer-Manz, G., Struhalla, G., van den Berg, L., Kiefer, D., Dalbey, R., and Kuhn, A. (2004). *Escherichia coli* YidC is a membrane insertase for Sec-independent proteins. EMBO J. *23*, 294–301.

Szyrach, G., Ott, M., Bonnefoy, N., Neupert, W., and Herrmann, J.M. (2003). Ribosome binding to the Oxa1 complex facilitates co-translational protein insertion in mitochondria. EMBO J. *22*, 6448–6457.

Urbanus, M.L., Scotti, P.A., Froderberg, L., Saaf, A., de Gier, J.W., Brunner, J., Samuelson, J.C., Dalbey, R.E., Oudega, B., and Luirink, J. (2001). Sec-dependent membrane protein insertion: sequential interaction of nascent FtsQ with SecY and YidC. EMBO Rep. *2*, 524–529.

Urbanus, M.L., Froderberg, L., Drew, D., Bjork, P., de Gier, J.W., Brunner, J., Oudega, B., and Luirink, J. (2002). Targeting, insertion, and localization of *Escherichia coli* YidC. J. Biol. Chem. *277*, 12718–12723.

Valle, M., Sengupta, J., Swami, N.K., Grassucci, R.A., Burkhardt, N., Nierhaus, K.H., Agrawal, R.K., and Frank, J. (2002). Cryo-EM reveals an active role for aminoacyl-tRNA in the accommodation process. EMBO J. *21*, 3557–3567.

van Bloois, E., Nagamori, S., Koningstein, G., Ullers, R.S., Preuss, M., Oudega, B., Harms, N., Kaback, H.R., Herrmann, J.M., and Luirink, J. (2005). The Sec-independent function of *Escherichia coli* YidC is evolutionary-conserved and essential. J. Biol. Chem. *280*, 12996–13003.

van Bloois, E., Koningstein, G., Bauerschmitt, H., Herrmann, J.M., and Luirink, J. (2007). *Saccharomyces cerevisiae* Cox18 complements the essential Sec-independent function of *Escherichia coli* YidC. FEBS J. *274*, 5704–5713.

van Bloois, E., Dekker, H.L., Froderberg, L., Houben, E.N., Urbanus, M.L., de Koster, C.G., de Gier, J.W., and Luirink, J. (2008). Detection of cross-links between FtsH, YidC, HflK/C suggests a linked role for these proteins in quality control upon insertion of bacterial inner membrane proteins. FEBS Lett. *582*, 1419–1424.

Van den Berg, B., Clemons, W.M., Jr., Collinson, I., Modis, Y., Hartmann, E., Harrison, S.C., and Rapoport, T.A. (2004). X-ray structure of a protein-conducting channel. Nature *427*, 36–44.

van der Laan, M., Houben, E.N., Nouwen, N., Luirink, J., and Driessen, A.J. (2001). Reconstitution of Sec-dependent membrane protein insertion: nascent FtsQ interacts with YidC in a SecYEG-dependent manner. EMBO Rep. *2*, 519–523.

van der Laan, M., Urbanus, M.L., Ten Hagen-Jongman, C.M., Nouwen, N., Oudega, B., Harms, N., Driessen, A.J., and Luirink, J. (2003). A conserved function of YidC in the biogenesis of respiratory chain complexes. Proc. Natl. Acad. Sci. USA *100*, 5801–5806.

van der Laan, M., Bechtluft, P., Kol, S., Nouwen, N., and Driessen, A.J. (2004). F1F0 ATP synthase subunit c is a substrate of the novel YidC pathway for membrane protein biogenesis. J. Cell Biol. *165*, 213–222.

van Heel, M., and Frank, J. (1981). Use of multivariate statistics in analysing the images of biological macromolecules. Ultramicroscopy *6*, 187–194.

van Heel, M., Harauz, G., Orlova, E.V., Schmidt, R., and Schatz, M. (1996). A new generation of the IMAGIC image processing system. J. Struct. Biol. *116*, 17–24.

Vinayagam, A., Pugalenthi, G., Rajesh, R., and Sowdhamini, R. (2004). DSDBASE: a consortium of native and modelled disulphide bonds in proteins. Nucleic Acids Res. *32*, D200–D202.

Yu, Z., Koningstein, G., Pop, A., and Luirink, J. (2008). The conserved third transmembrane segment of YidC contacts nascent *Escherichia coli* inner membrane proteins. J. Biol. Chem. *283*, 34635–34642.

Yuan, J., Phillips, G.J., and Dalbey, R.E. (2007). Isolation of cold-sensitive yidC mutants provides insights into the substrate profile of the YidC insertase and the importance of transmembrane 3 in YidC function. J. Bacteriol. *189*, 8961–8972.